Waste Management 117 (2020) 93–103

Contents lists available at ScienceDirect

Waste Management

journal homepage: www.elsevier.com/locate/wasman

PFOA and PFOS diffusion through LLDPE and LLDPE coextruded with EVOH at 22 °C, 35 °C, and 50 °C

V. Di Battista [a], R. Kerry Rowe [a,*], D. Patch [b], K. Weber [b]

[a] GeoEngineering Centre at Queen's – RMC, Queen's University, Kingston K7L 3N6, Canada
[b] Environmental Sciences Group, Department of Chemistry and Chemical Engineering, Royal Military College of Canada, Kingston, ON K7K 7B4, Canada

ARTICLE INFO

Article history:
Received 30 April 2020
Revised 7 July 2020
Accepted 15 July 2020

Keywords:
PFAS
PFOA
PFOS
Geomembranes
Diffusion
EVOH
LLDPE
Polyethylene

ABSTRACT

Diffusion of perfluorooctanoate (PFOA) and perfluorooctane sulfonate (PFOS) through 0.1 mm and 0.75 mm LLDPE and 0.1 mm and 0.75 mm LLDPE coextruded with ethyl vinyl alcohol (denoted as CoEx) at room temperature (23 °C), 35 °C, and 50 °C is examined. These tests had negligible source depletion throughout the monitoring period, indicating limited contaminant partitioning and diffusion through the LLDPE. At 483 days, 23 °C receptor PFOA and PFOS concentrations, c_r, were <8 μg/L ($c_r/c_o < 3.2 \times 10^{-4}$) for all tests, and at 399 days elevated temperature receptor concentrations were < 0.4 μg/L ($c_r/c_o < 1.6 \times 10^{-5}$) at 35 °C and <0.5 μg/L ($c_r/c_o < 2.0 \times 10^{-5}$) at 50 °C for both PFOA and PFOS. LLDPE partitioning coefficient, S_{gf} was 0.9–1.4 (PFOA) and 2.8–5.3 (PFOS) based on sorption tests at 23 °C. Based on the best estimates of permeation coefficient, P_{gCoEx}, for CoEx was consistently lower than P_{gLLDPE}. For PFOA, CoEx had $P_{gCoEx} < 0.26 \times 10^{-16}$ m^2/s at 23 °C, $<11 \times 10^{-16}$ m^2/s (35 °C), and $< 10 \times 10^{-16}$ m^2/s (50 °C) while LLDPE had $P_{gLLDPE} < 3.1 \times 10^{-16}$ m^2/s (23 °C), $<13 \times 10^{-16}$ m^2/s (35 °C), and $<19 \times 10^{-16}$ m^2/s (50 °C). For PFOS, CoEx and LLDPE had $P_{gCoEx} < 0.55 \times 10^{-16}$ m^2/s and $P_{gLLDPE} < 3.2 \times 10^{-16}$ m^2/s (23 °C), $P_{gCoEx} < 8.3 \times 10^{-16}$ m^2/s and $P_{gLLDPE} < 40 \times 10^{-16}$ m^2/s (35 °C), and $P_{gCoEx} < 8.2 \times 10^{-16}$ m^2/s and $P_{gLLDPE} < 52 \times 10^{-16}$ m^2/s (50 °C). These values are preliminary and may change (e.g., decrease) as more data comes available over time. The P_g values deduced for PFOA and PFOS are remarkably lower than those reported for other contaminants of concern, excepting BPA, which exhibits similar behaviour.

1. Introduction

Per- and polyfluoroalkyl substances (PFAS) are organofluoride alkyl molecules, typically 4–16 carbon atoms in length, with multiple fluorine atoms attached to the carbon chain. The C—F bond, which is extremely stable, gives these compounds desirable properties such as chemical and thermal stability (Buck et al., 2011). These substances have surfactant properties due to their hydrophilic functional end groups and hydrophobic fluorinated tail (3M Company, 1999a). Many consumer products contain PFAS as the stability of the molecules provide desirable properties allowing the chemicals to be used as protective coatings to textiles, papers, and packaging and to enhance the performance of various consumer products (3M Company, 1999b). There are over 4000 chemicals classified as PFAS, but the most widely studied PFAS compounds, perfluorooctanoate, $C_7F_{15}COOH$ (PFOA) and perfluorooctane sulfonate, $C_8F_{17}SO_3H$ (PFOS) are known to be persistent environmental contaminants due to the bioaccumulative, potentially carcinogenic, toxic properties of these compounds, and the chemical and thermal stability of the C—F bonds, (Gallen et al., 2017; Health Canada, 2018a,b; National Institute of Health Sciences, 2020). The major manufacturers of PFOA and PFOS have ceased production of these compounds in favour of alternative compounds (3M Company, 2000; Buck et al., 2011).

Historically, PFOA has been primarily used in manufacturing of fluoropolymers, including polytetrafluoroethylene. PFOS and other perfluorooctanesulfonyl fluoride based chemicals were used in surface treatments of textiles (e.g., carpets, upholstery, apparel, leather), paper and packaging protectors (e.g., grease repellent paper for food), and performance chemicals (e.g., coatings and coating additives, insecticides, etc.) (3M Company, 1999b; Buck et al., 2011; Martin et al., 2010). PFOS was a main component of aqueous film forming foam (AFFF) before production of PFOS was discontinued in North America. AFFF was primarily used for suppressing hydrocarbon fuel fires and fire combat training activities (Milley et al., 2018). Fire suppression and training activities at locations where large amounts of fuel are stored, such as airports, have resulted in PFAS contamination of the surrounding soil; a common

---

* Corresponding author.
E-mail addresses: v.di.battista@queensu.ca (V. Di Battista), kerry.rowe@queensu.ca (R.K. Rowe), David.Patch@rmc.ca (D. Patch), Kela.Weber@rmc.ca (K. Weber).

https://doi.org/10.1016/j.wasman.2020.07.036
0956-053X/

Nomenclature

List of notations

c	Concentration [mg L^{-1}]
D_g	Diffusion Coefficient [m^2 s^{-1}]
f	Diffusive flux [mg m^{-2} s^{-1}]
H	Membrane thickness [M]
log K_{ow}	n-octanol/water partition coefficient (–)
M	Mass [g]
M_w	Molar Mass [g mol^{-1}]
P_g	Permeability Coefficient [m^2 s^{-1}]
pK_a	Acid dissociation constant (–)
S_{gf}	Partitioning Coefficient (–)
V	Volume [L^3]
Z	Distance [Length]
r_g	Geomembrane Density [g cm^{-3}]

List of abbreviations

AFFF	Aqueous film forming foam
BPA	Bisphenol-A
BTEX	Benzene, toluene, ethylbenzene, xylenes
CMC	Critical micelle concentration
CoEx	Coextruded geomembrane (polyethylene/tie layer/EVOH/tie layer/polyethylene)
COV	Coefficient of Variation
DDI	Double De-Ionized
EVOH	Ethylene vinyl alcohol
HDPE	High density polyethylene
LLDPE	Linear low density polyethylene
MSW	Municipal Solid Waste
PBDE	Polybrominated diphenyl ethers
PCB	Polychlorinated biphenyl
PFAS	Per- and polyfluoroalkyl substances
PFOA	Perfluorooctanoate
PFOS	Perfluorooctane sulfonate
TCE	Trichloroethylene

remediation strategy for PFAS contaminated soil is excavation and placement in a landfill or monofill for contaminant containment (Hale et al., 2017).

Landfills are the ultimate destination for many consumer products, including those containing PFAS, and degradation of waste and water percolation through the landfill results in leachate containing PFAS, including PFOA and PFOS (Busch et al., 2010; Eggen et al., 2010; Fuertes et al., 2017; Gallen et al., 2017; Yan et al., 2015). Although manufacturing of PFOA and PFOS has been phased out, disposal of products containing these chemicals and contaminated soil remain a source of potential indirect release to the environment from landfills (Government of Canada, 2012). As leachate collects on the base of the landfill, the chemicals can migrate through the landfill liner, via advective and diffusive processes, and contaminate the surrounding environment (Rowe, 2015; Rowe et al., 2004). Specific chemical composition of landfill leachates is largely dependent on the waste source, composition of the landfill, and the age of the landfill (Rowe et al., 2004).

These chemicals are present in landfill leachates worldwide due to the ubiquity of PFOA and PFOS in consumer products. A study of six untreated German landfill leachates found that PFOA and PFOS accounted for 12% and 2.7% of the total PFAS in the leachates; the mean total PFAS concentration of the leachates was 6086 ng/L (Busch et al., 2010). Untreated municipal solid waste landfill leachate samples from four sites in northern Spain contained PFOA with concentrations ranging from 387 to 512 ng/L and accounted for an average of 42.6% of the total mass fraction of PFAS; PFOS concentrations in the landfill leachate ranged from below limit of detection to 43.5 ng/L (Fuertes et al., 2017). Eggen et al. (2010) sampled two landfills with clay liners and found that PFOS and PFOA accounted for 20–47% and 12–24% of total PFAS in the untreated landfill leachate, respectively; total PFAS concentrations were 2191–6123 ng/L in the leachate. Another study found that leachate sampled from a MSW landfill between February 2010 and June 2010 had variable levels of the specific PFAS species with PFOA and PFOS concentrations ranges of 300–1500 ng/L and 220–4400 ng/L, respectively, for untreated leachate that has not been recirculated in the landfill (Benskin et al., 2012). A study of 27 Australian landfills of various ages and stages of closure found PFOA and PFOS present in all 27 landfills, with mean concentrations of 690 ng/L and 310 ng/L, respectively, and maximum PFOA and PFOS concentrations as 7500 ng/L and 2700 ng/L, respectively (Gallen et al., 2017). Sampling of five untreated landfill leachates in China found total PFAS concentrations ranging from 7280 to 292,000 ng/L, with PFOA accounting for a mean of 36.8% (Yan et al., 2015).

The presence of these contaminants in landfills of various ages and locations highlights the need to understand the factors affecting their transport through the landfill liner components. The ability of the landfill to contain these contaminants depends on the existing liner system. Common materials used as liners are geomembranes, sheets of polyethylene 1.0–2.0 mm thick. Geomembranes are used worldwide for contaminant containment in landfills, and provide an advective barrier for contaminant migration such that molecular diffusion is the dominant contaminant transport mechanism (Rowe et al., 2004).

Multiple factors impact a geomembrane's diffusive characteristics. These factors are influenced by properties of the contaminant and geomembranes. One critical factor is the similarity (i.e., polarity and hydrophobicity) of the contaminant to the geomembrane, such that contaminant species will impact the diffusivity through a polyethylene geomembrane. In general, acids will have lower permeation coefficients than nitroderivatives, aldehydes, ketones, esters, ethers, and aromatic and chlorinated hydrocarbons. Benzene, toluene, ethylbenzene, xylenes (BTEX), and trichloroethylene can easily diffuse through polyethylene geomembranes due to the similarity in polarity of the polyethylene and the contaminants (August and Tatzky, 1984; Park et al., 1995; Park and Nibras, 1993; Rowe et al., 2004; Sangam and Rowe, 2001; Sangam and Rowe, 2005). Organic contaminants with greater n-octanol/water coefficients (log K_{ow}), a measure of hydrophobicity, and molecular weights (M_w) are more likely to partition to polyethylene, and greater molecular weights will reduce the diffusion coefficients (Park and Nibras, 1993; Rowe et al., 2004; Sangam and Rowe, 2001). PFOA and PFOS are neither hydrophobic or hydrophilic as their surfactant properties results in collecting at interfaces between aqueous and non-aqueous fluids. The log K_{ow} values for PFOA and PFOS have not been measured experimentally, but various investigators have estimated log K_{ow} values for these compounds from correlations with other properties of the compound (Arp et al., 2006; Rayne and Forest, 2009). The United States Environmental Protection Agency (US EPA) Industry Interface Estimation Suite uses atom/fragment contribution method to estimate log K_{ow} (US EPA, 2012). This computer program predicts log K_{ow} values of 4.81 (PFOA) and 4.49 (PFOS). This is within the ranges of log K_{ow} values predicted using other software tools (Arp et al., 2006; Rayne and Forest, 2009).

Alternative materials are used in conjunction with polyethylene to provide additional diffusive resistance to common landfill leachate contaminants (e.g., BTEX). Ethylene vinyl alcohol (EVOH), a co-polymer of ethylene and vinyl alcohol, is a hydrophilic substance that has high diffusive resistance to gases and organic compounds, such as BTEX and TCE (Lagaron et al., 2001; McWatters and Rowe, 2014, 2018; Eun et al., 2017). The hydrophilic nature of EVOH results in lower diffusion and partitioning coefficients of non-polar organic contaminants, compared to polyethylene, and geomembranes are being manufactured with EVOH cores coextruded with polyethylene outer layers as mitigation against vapour intrusion (McWatters et al., 2019; McWatters and Rowe, 2009, 2010, 2014). This EVOH layer decreases diffusive flux of contaminants through the geomembrane, and inclusion of an 0.0254 mm EVOH layer in a 0.5 mm geomembrane can reduce the steady state flux through a geomembrane for benzene by a factor of 19.5, compared to a 1.5 mm HDPE geomembrane (Di Battista and Rowe, 2020).

The primary objective of this study is to assess the diffusive behaviour of PFOA and PFOS through LLDPE and LLDPE coextruded with EVOH. This information is used to compare the diffusive properties of PFOA and PFOS to other known contaminants of concern.

2. Background

Diffusion is driven by the concentration gradient between two points, and Fick's first law calculates the steady state diffusive flux (f [ML^{2}T^{-1}] between two points (z) of a geomembrane for a one-dimensional system (Crank, 1979).

$$f = -D_g \frac{dc_g}{dz} \tag{1}$$

where D_g is the diffusion coefficient of the material [L^{2}T^{-1}], c_g is geomembrane concentration [ML^{-3}], and c_g [ML^{-3}] is the change in concentration over a small distance, dz [L]. Fick's first law cannot describe the transient aspect diffusion, and Fick's (so called) second law gives the change in concentration with time t.

$$\frac{\partial c_g}{\partial t} = D_g \frac{\partial^2 c_g}{\partial z^2} \tag{2}$$

Fick's laws are used to calculate diffusion within a geomembrane. However, when the contaminant in is an aqueous solution in contact with the geomembrane, the contaminant undergoes a phase change when partitioning from the aqueous solution (e.g., a source reservoir) into the polymer. This phase change is expressed using the partitioning coefficient S_{gf} (–), which is calculated as the ratio of the geomembrane concentration to the fluid concentration using a modified Henry's Law.

$$c_g = S_{gf} c_f \tag{3}$$

Under steady state conditions, Eq. (3) can be substituted into Fick's first law such that when there is a constant concentration gradient between the source to receptor equal to the difference in concentration between the two sides of the geomembrane (Δc_f) divided by the geomembrane thickness (H), the mass flux, f, through the geomembrane is given by:

$$f = -D_g \frac{dc_g}{dz} = -S_{gf} P_g \frac{dc_f}{dz} = -P_g \frac{\Delta c_f}{H} \tag{4}$$

Thus, a permeation coefficient, P_g, can be calculated as the product of D_g and S_{gf}.

3. Materials and methods

Four geomembranes were used in this study, 0.1 mm LLDPE, 0.1 mm LLDPE coextruded with a 0.01 mm layer of EVOH (0.1 mm CoEx), 0.75 mm LLDPE, and 0.75 mm LLDPE coextruded with 0.03 mm EVOH (0.75 mm CoEx). Experiments were conducted at room temperature (23 °C) and in ovens set at 35 °C and 50 °C. Cells containing the four geomembranes are currently running at 23 °C, and elevated temperature testing was initiated for the 0.1 mm LLDPE, 0.75 mm LLDPE, and the 0.75 mm CoEx.

Based on Fick's first law, the diffusive flux through a geomembrane is inversely proportional to the membrane thickness. Anticipating that D_g may be low for PFAS and PFOA, the tests were initiated with membranes thinner than the 1.5–3 mm thickness geomembrane typically used in landfill to allow greater diffusion in a shorter time period. The ratio, P_g/H, and the ratio D_g/H can be used to estimate the parameters for thicker geomembranes. Also, HDPE is more commonly used in landfills than LLDPE, but it is known that diffusion coefficient through polyethylene geomembranes generally decreases with higher crystallinity due to a greater tortuosity of the diffusive path through the amorphous zone and around the polyethylene crystals (Islam and Rowe, 2009). Since LLDPE has a lower crystallinity than HDPE, results from experiments using LLDPE will likely give a conservative estimate for the diffusion coefficients for HDPE (Jones and Rowe, 2016).

Stainless steel double compartment diffusion cells were used in this study. These cells have a source and receptor separated by the geomembrane with volumes of 465 ml (source) and 180 ml (receptor). Similar studies of BTEX diffusion used Viton gaskets to obtain seals between the membrane and the cell (Jones, 2016; McWatters, 2010; McWatters and Rowe, 2018). However, the Viton gaskets, a fluoride copolymer, typically used were replaced with silicone gaskets of the same size to avoid a possible contamination of the cells. Clean cell components were rinsed with 10 ml of 0.1% ammonium hydroxide in methanol; the rinsate concentrations were below detection for PFOA and PFOS.

The stock solutions were mixed using 1 g PFOS (97% purity) and 1 g PFOA (98% purity), purchased from Synquest Laboratories (Aluchua, Florida). The PFOA and PFOS were added to 2 L and 1 L volumetric flasks with DDI water, respectively, to create separate solutions of 500 mg/L PFOS and 1000 mg/L PFOA. The concentrations of these solutions were analyzed and confirmed. These stock solutions were used to create all source solutions used in the experiments. The diffusion cells had initial source concentrations, c_o, of 19.8 mg/L (PFOA) and 22.7 mg/L (PFOS) to create a large diffusion gradient and increase diffusive flux through the membrane. These concentrations well below the solubility limits at room temperature (2290–4340 mg/L for PFOA and 519–680 mg/L for PFOS) and critical micelle concentration (CMC) of aqueous PFOA (~15,700 mg/L) and PFOS (~4570 mg/L), and it is unlikely that micelle formation will occur in solution. However, the formation of hemi-micelles can occur in aqueous concentrations as high as 0.01–0.001 times the CMC (Johnson et al., 2007; Yu et al., 2008). To assess the impacts of potential hemi-micelle formation on the source concentrations or diffusive processes (if any), additional experiments using the 0.1 mm LLDPE at 23 °C, 35 °C, and 50 °C were initiated with initial PFOA and PFOS concentrations of 1.1 mg/L (below 0.0001CMC for PFOA and 0.001CMC for PFOS).

Sampling was performed using separate syringes for the source and receptors to decrease chances of contamination. To sample the cells, a small volume (<200 µl) was removed from the source or receptor and replaced with an equal volume of DDI water. Syringes were then rinsed three times with methanol and DDI water before the next use. Syringe and water blanks were analyzed before experiments began and randomly during the experimental process to ensure results were not influenced by contamination.

Sorption experiments using the 0.75 mm LLDPE were also initiated. These experiments were prepared by creating a source solution of 376 μg/L, and this solution was decanted into two vials containing geomembrane and a third control vial with no geomembrane. An initial sample of the solution was extracted before the solution was decanted into the individual vials to confirm initial concentration.

All samples were analyzed on an Agilent 6460 LC-MS/MS running in MRM mode. Separation was performed using a 150 mm × 2.1 mm × 3.0 um Zorbax C18 Eclipse Column coupled with guard column. Samples were eluted over a 10 min period, starting at 95% water (10 mM ammonium acetate) and 5% acetonitrile, transitioning to 100% acetonitrile over 8 min, then holding at 100% acetonitrile for the last 2 min. The column was then re-equilibrated at original elution conditions for 4 min before the next sample analysis.

Concentrations were calculated using an eight point calibration curve across 0.01 μg/: to 200 μg/L (0.01, 0.1, 1, 5, 10, 50, 100, 200). The varying concentrations of calibration standards were made from standards purchased from Wellington Laboratories. Two double injection blanks (methanol) were run before each method blank, reagent blank, calibration curve, post-treatment sample, and experimental blanks to eliminate contamination and carry-over from other samples. The reporting limit for analyses was 0.1 μg/L. Syringe blanks and water blanks were included in the analysis and at sporadic dates throughout the test durations

4. Results

4.1. Diffusion testing

Diffusion tests conducted at 23 °C for the four geomembranes have sampling data available up to 483 days. In this time there has been limited observed permeation of the contaminants through the 0.1 mm LLDPE, 0.1 mm CoEx, 0.75 mm LLDPE, and 0.75 mm CoEx. The initial source concentrations for these tests were c_o = 19.8 mg/L (PFOA) and c_o = 22.7 mg/L (PFOS). Source concentrations of PFOA and PFOS for the 0.75 mm LLDPE, 0.75 mm CoEx, 0.1 mm LLDPE, and 0.1 mm CoEx were scattered about the initial value of the source concentrations (Fig. 1), and unlike organic contaminants, there was no pattern of decrease discernable from the scatter over the entire period of monitoring. The scatter requires some explanation. The data over the first 180 days was obtained by analysis from a commercial lab that took no special care (i.e., they were analyzed as routine samples with no additional dilution). These samples had a dilution factor of 15 before being sent for analysis, and the reported concentrations were >10,000 μg/L. The highest point on the calibration curves were 625 μg/L (PFOS) and 312 μg/L (PFOA). Samples analyzed after 180 days, were analyzed by a specialized lab, and samples were diluted to fall within the maximum point of the calibration curve (200 μg/L). These samples had high dilution factors (~50), which can magnify any analytical uncertainty. Special attention was paid to obtaining the last data point and it showed minimal decreases and remained close to c/c_o = 1. The short-term stability in the source concentrations indicate that little to no partitioning of the contaminants to the LLDPE is occurring, and the long-term stability of the source concentrations indicates that minimal diffusion had occurred over the period monitored, as significant mass flux through the geomembrane would notably and consistently decrease the source concentration in the 483–509 days of testing reported herein. The average source concentrations for the cells were 19.5 mg/L (n = 37, σ = 2.5 mg/L) for PFOA and 24.2 mg/L (n = 36, σ = 5.3 mg/L), for PFOS. Given the magnitude of the standard deviation, σ, the differences in mean concentrations of the individual cells (LLDPE vs CoEx) were not statistically significant (p < 0.1), and the initial concentration was within the 99% confidence intervals calculated for the individual cells. There was no discernible (measurable) decrease in source concentration with time. If the contaminants were partitioning into the geomembrane, as would occur for BTEX or many other organic compounds, or lost to the environment through leakage in the cell gaskets and septa, the individual cell means and population mean would be lower. These conclusions, based on source data alone, are consistent with data from the receptor concentrations and sorption test data for LLDPE discussed below. Although there is uncertainty regarding the precise source concentration, due to the very large difference in source and detected receptor concentrations this uncertainty has a relatively little effect on the diffusion and permeation coefficients, as illustrated later.

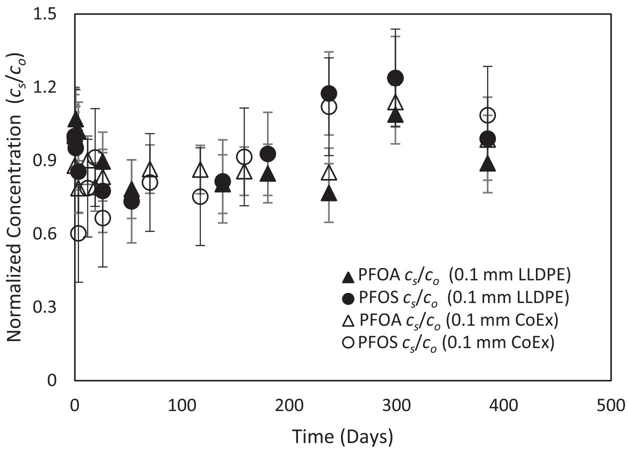

Fig. 1. Normalized source concentrations, c_s/c_o, for 0.1 mm LLDPE and CoEx at room temperature; c_o = 19.8 mg/L (PFOA) and c_o = 22.7 mg/L (PFOS).

Receptor samples had no need for dilution prior to analysis, and the receptor concentrations will be the primary experimental data used for developing estimates of the diffusion and permeation coefficients for the materials tested.

Excluding the effects of analytical variability and uncertainty, due to a larger diffusion gradient across the 0.1 mm LLDPE compared to the 0.75 mm LLDPE, contaminant detection for the 23 °C experiments is expected to occur earlier for 0.1 mm geomembranes due to the larger diffusion gradient compared to the 0.75 mm LLDPE, and at a given time after breakthrough, the concentration would be greater prior to equilibrium for the 0.1 mm than the 0.75 mm GMB. Also, if the diffusion coefficient for these compounds is lower for EVOH than LLDPE, detection of PFOA and PFOS would be expected to occur earlier for LLDPE than for the CoEx of the same thickness; at a given time after breakthrough, the receptor concentration would be higher prior to equilibrium. Indeed, the first receptor concentration to exceed the detection limit was the 0.1 mm LLDPE at 299 days (c_{PFOA} = 0.4 μg/L and c_{PFOS} = 0.7 μg/L). Receptor concentrations above detection were observed later (at 334 days) for the 0.1 mm CoEx (c_{PFOA} = 0.6 μg/L and c_{PFOS} = 2.6 μg/L). Even with no dilution, it was found that there was notable scatter in the receptor data and it is difficult discern a clear trend of increasing concentration with time in the experiments (Fig. 2). The concentrations obtained with subsequent sampling for these cells have been very low ($c_{PFOA} \leq 0.6$ μg/L and $c_{PFOS} \leq 0.8$ μg/L) indicating diffusion is occurring extremely slowly. The most recent sampling data (Supplementary Material Table S1), at 483 days, had receptor concentrations of c_{PFOA} = 0.3 μg/L and

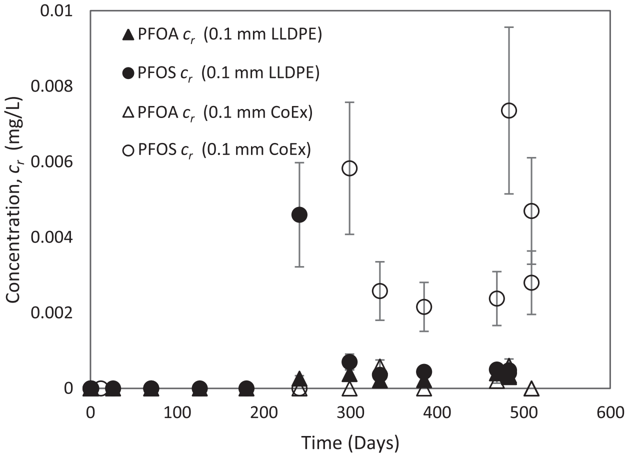

Fig. 2. Receptor concentrations, c_r, (detection limit = 0.0001 mg/L) for 0.1 mm LLDPE and 0.1 mm CoEx at 23 °C; c_o = 19.8 mg/L (PFOA) and c_o = 22.7 mg/L (PFOS).

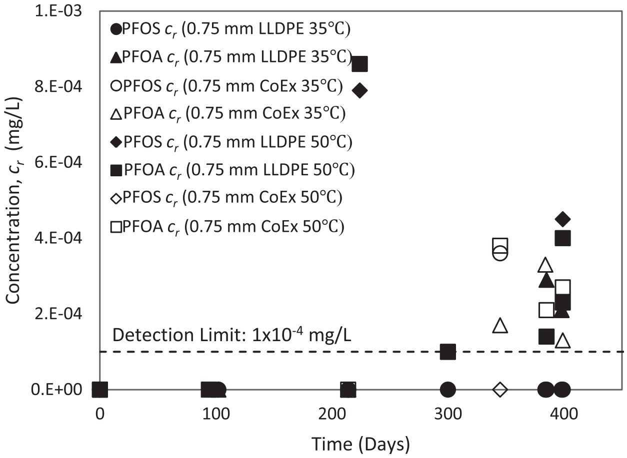

Fig. 3. Receptor concentrations, c_r, for 0.75 mm LLDPE and 0.75 mm CoEx at 50 °C; c_o = 19.8 mg/L (PFOA) and c_o = 22.7 mg/L (PFOS).

c_{PFOS} = 0.5 μg/L (0.1 mm LLDPE) and below detection for both PFOA and PFOS (0.1 mm CoEx). In comparison, if benzene (D_g = 2.2 × 10^{-13} m^2/s S_{gf} = 200; Di Battista and Rowe, 2020) was the contaminant of interest, an equilibrium would be reached in 31 days (c_{eq} = 18.9 mg/L) for the 0.1 mm LLDPE geomembrane using an identical experiment set-up (c_o = 22 mg/L).

Detection of PFOA in the 0.75 mm LLDPE at 23 °C occurred at 299 days (1.4 μg/L), and detection of PFOS occurred at 429 days (0.3 μg/L). The most recent sampling (509 days) were below detection for PFOA and PFOS; in contrast a diffusion test with c_o = 22.7-mg/L benzene in an identical cell would reach equilibrium in 77 days (c_{eq} = 10.3 mg/L) for 0.75 mm LLDPE. Detection of PFOA in the 0.75 mm CoEx receptor samples occurred at 469 days (0.3 μg/L), and PFOS concentrations have remained below detection for the duration of testing.

Permeation of contaminants through geomembranes increases with temperature. Elevated temperature experiments (at 35 °C and 50 °C) with c_o = 19.8 mg/L (PFOA) and c_o = 22.7 mg/L (PFOS) were initiated to assess the effect of temperature on the diffusion of PFOA and PFOS through the 0.75 mm LLDPE and CoEx geomembranes, however even at these temperatures very limited permeation of contaminants has been observed in the testing duration. Similar to the 23 °C experiments, there has been no discernible depletion in the source concentrations for these elevated temperature tests (e.g., at 50 °C in Supplementary Material Fig. S1) with the analyzed concentrations of the 0.75 mm LLDPE experiment at 50 °C averaging 22.4 mg/L (n = 7, σ = 2.6 mg/L) for PFOA (c_o = 19.8 mg/L) and 27.2 mg/L (n = 7, σ = 5.4) for PFOS (c_o = 22.1 mg/L). At the most recent sampling event (399 days), receptor concentrations for the 0.75 mm LLDPE at 50 °C were 0.4 μg/L (PFOA) and below quantification (PFOS) and 0.2 μg/L (PFOA) and below quantification (PFOS) at 35 °C (Fig. 3). The first sampling point above detection occurred at 224 days (c_{PFOA} = 0.9 μg/L and c_{PFOS} = 0.8 μg/L) for the 50 °C test, which is 75 days earlier than observed for the 0.75 mm LLDPE at 23 °C while PFOA was detected at 300 days (0.05 μg/L) in the 35 °C. PFOS concentrations have been below quantification for this experiment. Faster time to contaminant breakthrough is expected as diffusion will increase as temperature increases (Rowe et al., 2004). Although, the 50 °C experiment had contaminant breakthrough sooner, the mass flux through the LLDPE is still extremely low, even at the elevated temperatures, as evidenced by the lack of source depletion and low receptor concentrations at 399 days.

The 0.75 mm CoEx geomembrane had receptor concentrations of 0.3 μg/L (PFOA) and below detection (PFOS) in the 50 °C cell, and the 35 °C cell had receptor concentrations of 0.1 μg/L (PFOA) and below detection (PFOS) at 399 days (Fig. 3). Receptor PFOA concentrations were first above detection in the 50 °C experiment at 345 days (0.4 μg/L), and PFOS were above detection but below quantification. The 0.75 mm CoEx at 35 °C had receptor detectable receptor concentrations at 345 days (c_{PFOA} = 0.2 μg/L and c_{PFOS} = 0.4 μg/L). Contaminant breakthrough was observed sooner in the LLDPE tests than in the CoEx tests for the 23 °C, 35 °C and 50 °C tests, indicating that the EVOH core may provide greater diffusive resistance to PFOA and PFOS diffusion than the LLDPE.

The three cells with c_o = 1.1 mg/L for PFOA and PFOS at 23 °C, 35 °C, and 50 °C have sample data available up to 202 days. Similar to the experiments using c_o > 20 mg/L, the 1.1 mg/L source concentrations did not exhibit any discernable decreases, and receptor concentrations were below detection for PFOA and PFOS at the 202 day sampling point. Similar observed behaviour in the source of c_o = 1.1 mg/L and c_o > 20 mg/L indicate that hemi-micelle formation on the cell walls or geomembrane surface (if present) is not discernably affecting the initial stages of diffusion through the geomembrane, however these tests will remain active for future monitoring.

4.2. Room temperature sorption testing

Sorption tests were conducted with LLDPE at 23 °C with c_o = 263-μg/L for both PFOA and PFOS (c_o < 0.0001CMC); a control test with no geomembrane was also assembled at the same time. These tests have been active for 226 days, and there have been small decreases in PFOA and PFOS concentrations observed in the vials containing the LLDPE compared to the control vial. Using the mass balance of the sorption tests, S_{gf} can be calculated from

$$S_{gf} = \frac{\left[c_{f^\circ} V_{f^\circ} - c_{fF} V_{fF} - M_c\right]\rho_g}{M_g c_{gF}} \tag{5}$$

where c_{fo}, c_{fF}, c_{gF} denote initial and final aqueous concentrations and the final concentration of the geomembrane at equilibrium [ML^{-3}], respectively, and V_{fo} and V_{fF} denote initial and final solution volumes [L^3]. The geomembrane mass and mass of contaminant lost to the system (quantified using control tests) are expressed as M_g and M_c [M], respectively, and geomembrane density is denoted as ρ_g [L^{3}M].

Using Eq. (5), estimates of the partitioning coefficients were calculated: 0.9–1.4 (PFOA) and 2.8–5.3 (PFOS). These preliminary S_{gf} values support the limited source decreases observed in the diffusion experiments for c_o > 20 mg/L and c_o = 1.1 mg/L. These values are currently the best estimates, however despite the fact that these tests have been running a relatively long time, it is unlikely that they have reached equilibrium during the period of observation due the low diffusivity of PFOA and PFOS through LLDPE, as observed in the diffusion experiments. Monitoring of these experiments is ongoing.

4.3. Preliminary diffusion modelling

Using a the finite layer program POLLUTE v7(Rowe and Booker, 1985, 2004; Rowe et al., 1988, 1997; Barone et al., 1990, 1992a,b; Rowe and Badv, 1996; Rowe, 1998; Lake and Rowe, 2004; Sangam and Rowe, 2001; Rowe et al., 2005), best estimate diffusion coefficients were developed for LLDPE by modelling the receptor concentrations with time for the diffusion experiments. The D_g values were developed by matching a theoretical model to the receptor concentrations at the most recent sampling event. If receptor concentrations were below detection or quantification, such that no number could be assigned from the test, a concentration equal to the detection limit (0.1 μg/L) was used to obtain an upper bound on the diffusion coefficient for the value of S_{gf} inferred from the sorption test. Best estimate diffusion coefficients and consequent partitioning coefficients were inferred from the latest data point given the absence of any clear trend of an increase with time (Table 1), however the receptor concentrations are extremely low for all tests (<8 μg/L, c_r/c_o < 0.0004), and the diffusion/permeation coefficients reported may decrease further with the availability of new data and more time. For PFOA diffusing through 0.1 mm LLDPE, the best estimate is $D_g \leq 2.5 \times 10^{-17}$ m^2/s and $P_g \leq 3.1 \times 10^{-17}$ m^2/s and for PFOS the best estimate is $D_g \leq 4.0 \times 10^{-17}$ m^2/s and $P_g \leq 1.6 \times 10^{-16}$ m^2/s after 483 days at 23 °C.

The 23 °C partitioning coefficients were used to model the elevated temperature tests although the partitioning coefficients are likely to increase with temperature, however, the limited reductions in source concentrations for the tests at 35 °C and 50 °C indicate that there is limited contaminant partitioning occurring, even at the elevated temperatures. Preliminary best estimate diffusion coefficients have been proposed for the LLDPE at 23 °C, 35 °C, and 50 °C (Table 1). To illustrate the value of running tests longer, especially when receptor concentrations are below or near the detection limit, one can compare best estimates for P_g obtained from the 50 °C 0.75 mm LLDPE experiments; at 214 days, the best estimate $P_g \geq 3.8 \times 10^{-15}$ m^2/s compared to P_g > 1.4–1.9 × 10^{-15} m^2/s at 399 days, for PFOA and note the decrease by a factor of two. Due to the preliminary nature of these results (only 399 days testing at 35 and 50 °C) with the receptor concentrations near or below detection, no clear trend is evident in an Arrhenius plot of the natural logarithm of the best estimate permeation coefficients, P_g, plotted against the inverse of temperature (in K), 1/T, for the 0.75 mm LLDPE and CoEx membranes (Supplementary Material Fig. S2). LLDPE is an effective barrier to PFOA and PFOS, as evidenced by P_g values for LLDPE ranging from $\leq 5.2 \times 10^{-15}$ m^2/s (PFOS at 50 °C) to as low as $\leq 3.1 \times 10^{-17}$ m^2/s (PFOA at 23 °C).

The 0.1 mm material was tested because, for the same source and receptor properties and initial source concentrations, a contaminant diffusing through geomembranes of the same material but different thickness, will reach the receptor earlier for the thinner geomembrane. This is why the best estimate values reported for the 0.1 mm and the 0.75 mm LLDPE vary by more than an order of magnitude. Despite 509 days if testing, receptor concentrations for the 0.75 mm LLDPE were below detection or quantification (Supplementary Material Table S1). Thus, the P_g value has to be estimated based on the detection limit at 509 days. The longer the test is run and the receptor remains below the detection limit, the lower will be the estimate of P_g. Once the sampled receptor concentrations for the 0.1 mm and 0.75 mm LLDPE are consistently above the detection levels and there is a trend of increasing receptor concertation with time, the best estimate P_g for the 0.75 mm LLDPE will likely be similar to the values reported for the 0.1 mm LLDPE. That said, the P_g values for the 0.75 mm LLDPE (Table 1) are still very low. Nevertheless, as the 0.1 mm LLDPE experiments had more data points above detection during the monitoring period they are considered more representative of the actual P_g and so the following comparisons and discussion will be based on the best estimates provided for the 0.1 mm LLDPE.

Using the same a method to deduce D_g values for LLDPE, best estimate P_g values are proposed for the coextruded membranes based on the experiments 23 °C, 35 °C, and 50 °C (Table 1). Since there is no data available regarding diffusion of PFOA and PFOS through individual components of the system S_{gf} and D_g cannot be defined for the system. At 23 °C, best estimate P_g values for are $P_{gPFOA} \leq 2.6 \times 10^{-17}$ m^2/s and $P_{gPFOS} \leq 5.5 \times 10^{-17}$ m^2/s for the 0.1 mm CoEx (Fig. 4) and $P_{gPFOA} \leq 8.6 \times 10^{-16}$ m^2/s (PFOA) and $P_{gPFOS} \leq 6.8 \times 10^{-16}$ m^2/s (PFOS) for the 0.75 mm CoEx. The proposed parameters are current best estimates based on the limited receptor data arising from the remarkably low receptor concentrations despite relatively high values of c_o = 19.8 mg/L and c_o = 22.7 mg/L. To assess the effect of uncertainly due to the variability observed in the experimental data, P_g was also obtained by modelling the data for c_o values representative of the later time source data (i.e., c_o = 21.5 mg/L for PFOA and c_o = 26.9 mg/L for PFOS; Fig. 4), and the deduced values of P_g were not notably different from the original best estimates and the higher c_o actually results in a lower estimate of P_g.

Best estimate P_g values for the 0.75 mm CoEx ranged from $\leq 6.8 \times 10^{-16}$ m^2/s (PFOS 23 °C) to $\leq 1.1 \times 10^{-15}$ m^2/s (PFOA 35 °C). These values are based on the data available, and the proposed best estimates are likely to decrease as monitoring continues. Upper bound permeation coefficients could be developed such that the modelled concentrations match the date and concentration of the maximum analyzed concentration. This would be very conservative as, generally, the receptor concentrations have been oscillating above and below the detection limit for most cells. The estimated vales of P_g are likely to decrease as the test runs for a longer period of time, and will be more clearly defined when concentrations in

Table 1
PFOA and PFOS best estimate D_g, S_{gf}, and P_g values for LLDPE and CoEx membranes at multiple temperatures.

Material	Temp. (°C)	PFOA			PFOS		
		D_g ($\times 10^{-16}$ m^2/s)	S_{gf} (–)	P_g ($\times 10^{-16}$ m^2/s)	D_g ($\times 10^{-16}$ m^2/s)	S_{gf} (–)	P_g ($\times 10^{-16}$ m^2/s)
0.1 mm LLDPE	23	≤0.25	0.9–1.4	≤0.31	≤0.40	2.8–5.3	≤1.6
0.75 mm LLDPE	23	≤10	0.9–1.4	≤9–13	≤6.5–6.7	2.8–5.3	≤19–34
0.75 mm LLDPE	35	≤9.3–10	0.9–1.4	≤9–13	≤7.6–7.8	2.8–5.3	≤22–40
0.75 mm LLDPE	50	≤10–19	0.9–1.4	≤14–19	≤9.8–9.9	2.8–5.3	≤27–52
0.1 mm CoEx	23	–	–	≤0.26	–	–	≤0.55
0.75 mm CoEx	23	–	–	≤8.6	–	–	≤6.8
0.75 mm CoEx	35	–	–	≤11	–	–	≤8.3
0.75 mm CoEx	50	–	–	≤10	–	–	≤8.2

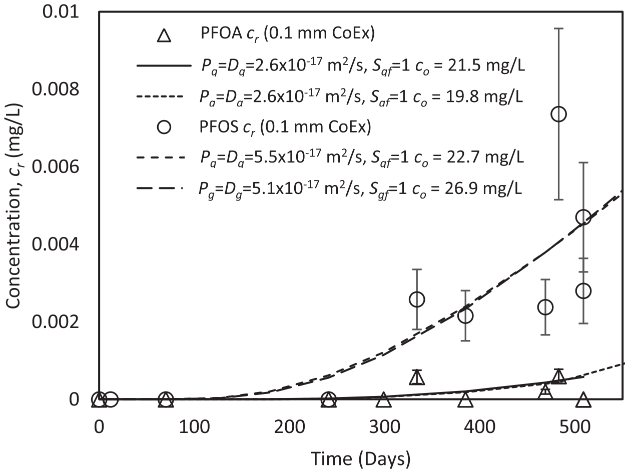

Fig. 4. PFOA Observed and calculated receptor concentrations, c_r, for 0.1 mm CoEx for both PFOA and PFOS at 23 °C. Two calculated curves are shown for each. One is for the initial source concentration (c_o = 19.8 mg/L for PFOA and c_o = 22.7 mg/L for PFOS) and the other for a representative value in the latter part of the test (c_o = 21.5 mg/L for PFOA and c_o = 26.9 mg/L for PFOS).

the receptor are consistently above the detection limit and show a clear trend of increasing with time. For comparable thicknesses, the CoEx consistently has similar or lower P_g values than the LLDPE alone.

5. Discussion

The best estimate parameters for the LLDPE and the coextruded geomembranes can be compared to diffusion parameters for polyethylene that have been proposed for a variety of contaminants that exist in landfill leachate (Table 2). Organic contaminants, specifically BTEX, have greater D_g, S_{gf}, and P_g values for LLDPE than PFOA and PFOS; this is, in part, likely due to smaller molecular weights, M_w, and greater hydrophobicity, of the BTEX compounds compared to PFOA and PFOS. Although the estimated log K_{ow} values for PFOA and PFOS are higher than those of BTEX (Table 2), their molecular structures result in molecules that have both lipophilic and hydrophilic properties, and the hydrophilic functional end groups are likely to decrease the ability of the contaminant to partition from an aqueous phase solution to the LLDPE (Rayne and Forest, 2009). Studies of other emerging contaminants with M_w > M_{wBTEX} have shown that polybrominated diphenyl ethers (PBDE) and polychlorinated biphenyl Aroclor 1242 (PCBs)s have extremely high S_{gf} values (>150,000) for HDPE, resulting in P_g values greater than the P_g values for BTEX, and S_{gf} values more than 30,000-fold greater than best estimates calculated for PFOA and PFOS (Table 2 and Rowe et al., 2016b,a). This is likely influenced by other chemical properties beside M_w, such as hydrophobicity. Bisphenol-A (BPA) and phenol are emerging contaminants that behave in a more similar manner to PFOA and PFOS, where little to no partitioning of the BPA and phenol into HDPE was observed, even though the calculated log K_{ow} value for BPA is greater than those of BTEX and its solubility is similar to or lower than BTEX (Supplementary Material Table S2) BPA has a very low S_{gf} value, and, over 1500 days of monitoring, there was limited source concentration decrease and receptor concentration increase for BPA (Saheli et al., 2016). When comparing the M_w of contaminants to their respective D_g values for polyethylene, PFOA and PFOS follow a similar trend as BTEX, PCBs, PBDE, BPA, and phenol and their respective D_g values for polyethylene (Fig. 5); as M_w increases, D_g decreases in an exponential fashion. The solubility of BPA (120–380 mg/L) with $S_{gf} \leq 1$ (too small to be measured reliably) and phenol (90,000 mg/L) with $S_{gf} \sim 3.5$ bracket those for PFOA (2290–4340 mg/L) and PFOS (519–680 mg/L; Supplementary Material Table S2) and so to the extent S_{gf} is related to solubility one would expect $1 \leq S_{gf} \leq 3.5$ for PFOA and PFAS; however S_{gf} depends on more than solubility. The topological polar surface areas [$\hat{A}^2$], a measure of surface area in a molecule from polar atoms, ranged from 20.2 $\hat{A}^2$ (phenol) to 62.8 $\hat{A}^2$ (PFOS). When compared with compounds with higher S_{gf} values, BTEX and PCBs have a topological surface area of 0 $\hat{A}^2$ while PBDE, which has S_{gf} = 1,800,000, has a topological surface area of 9.2 $\hat{A}^2$. Thus, while the polar surface area may be a contributing factor to the ability of a compound to partition to polyethylene, it too is unlikely to be the main predictor, based on the PBDE values. These complexities make it difficult to develop simple empirical relationships to predict S_{gf} as will be shown later.

Prior to this study, there was no available information regarding the diffusion parameters of PFOA and PFOS for polyethylene, but estimations for D_g, S_{gf}, and P_g could be calculated using correlations from the literature. Sangam and Rowe (2001) developed the following correlations using M_w, and log K_{ow} of organic contaminants to predict the P_g, D_g, and S_{gf} values for HDPE:

Table 2
PFOA and PFOS best estimate D_g, S_{gf}, and P_g values compared to literature values for other chemicals at room temperature.

Contaminant	log K_{ow} (–)	M_w (g/mol)	D_g (m^2/s)	S_{gf} (–)	P_g (m^2/s)
PFOA – CoEx 0.1 mm	4.81[e]	414.07	–	–	<2.6 × 10^{-17}
PFOS – CoEx 0.1 mm	4.49[e]	500.13			<5.5 × 10^{-17}
PFOA – LLDPE 0.1 mm	4.81[e]	414.07	<2.5 × 10^{-17}	0.9–1.4	<3.1 × 10^{-17}
PFOS – LLDPE 0.1 mm	4.49[e]	500.13	<4 × 10^{-17}	2.8–5.3	<1.6 × 10^{-16}
Benzene[a]	2.15[f]	78.11	2.2 × 10^{-13}	200	4.4 × 10^{-11}
Toluene[a]	2.73[f]	92.14	2.2 × 10^{-13}	350	7.7 × 10^{-11}
Ethylbenzene[a]	3.15[f]	106.17	1.0 × 10^{-13}	925	9.2 × 10^{-11}
m&p-Xylene[a]	3.15–3.2[f]	106.16	0.8 × 10^{-13}	900	7.2 × 10^{-11}
o-xylene[a]	3.16[f]	106.16	0.8 × 10^{-13}	900	7.2 × 10^{-11}
PCBs Aroclor 1242[b]	6.98[e]	291.98	5-50 × 10^{-15}	90,000–325,000	0.45-16 × 10^{-9}
BPA[c]	3.64[e]	228.29	–	–	2.9 × 10^{-15}
Phenol[c]	1.46[c]	94.11	1.7 × 10^{-14}	3.48	5.9 × 10^{-14}
PBDE (DE-71 Mixture)[d]	6.81–7.90[d]	564.7	4 × 10^{-15}	1,800,000	7.2 × 10^{-9}

[a] LLDPE (Di Battista and Rowe, 2020).
[b] HDPE (Rowe et al., 2016a).
[c] HDPE (Saheli et al., 2016).
[d] HDPE (Rowe et al., 2016b).
[e] Calculated using US EPA Industry Interface Estimation Suite (US EPA, 2012)
[f] Montgomery and Welkom (1989).

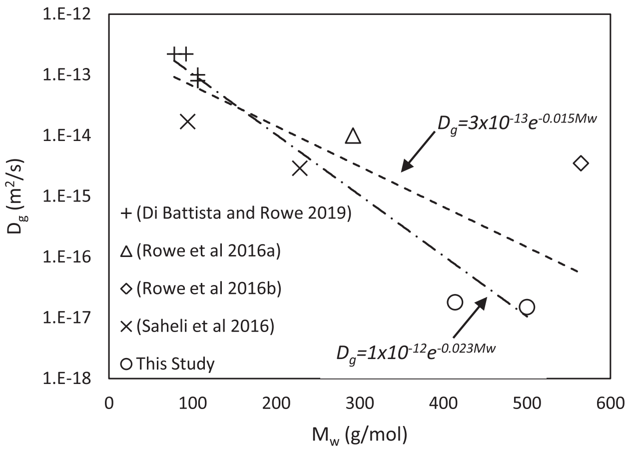

Fig. 5. Diffusion coefficient variation with molecular weight for various contaminants from this study and previous studies.

$$\log S_{gf} = -1.1523 + 1.2355(\log K_{ow}) \tag{R1}$$

$$\log P_g = -13.4476 + 2.2437(\log K_{ow}) - 0.3910(\log K_{ow})^2 \tag{R2}$$

$$\log P_g = -25.6933 + 0.2633 M_W - 1.0995 \times 10^{-3} \ (M_W)^2 \tag{R3}$$

$$\log D_g = -12.3624 + 0.9205 \log K_{ow} - 0.3424(\log K_{ow})^2 \tag{R4}$$

These correlations were developed using semi-empirical and empirical methods for contaminants with an affinity for polyethylene. Using Eqs. (R1), (R2), (R3), and (R4), D_g, S_{gf}, and $P_g$values can be calculated based on the contaminant properties of PFOA and PFOS and compared to the best estimate D_g, S_{gf}, and P_g values deduced from this study (Table 3). The authors recognize that the correlations were developed for contaminants with a high affinity for polyethylene using parameters reported for HDPE instead of LLDPE, and that the empirical predictions based on polymer class do not account for geomembrane specific factors affecting diffusion, (e.g. crystallinity within the range relevant to a class).

The S_{gf} values calculated using Eq. (R1) (61,000 for PFOA and 25,000 for PFOS) are many orders of magnitude greater than the best estimates calculated using the experimental data. These values are high, like the S_{gf} values calculated for PCBs (S_{gf} = 90,000) and PBDE (S_{gf} = 1,800,000), and would have resulted in rapid depletion of the source concentrations if true for PFOA and PFOS (Rowe et al., Rowe et al., 2016b,a). Since no discernible source depletion was observed in all tests, Eq. (R1) using log K_{ow} is not a suitable predictor of S_{gf} for PFOA and PFOS.

Eqs. (R2) and (R3) are correlations to calculate P_g using M_w and log K_{ow}, respectively. Values predicted by Eq. (R2) (2.0 × 10^{-12} m^2/s for PFOA and 5.5 × 10^{-12} m^2/s for PFOS) are comparable to P_g values reported for BTEX. Modelling of PFOA diffusion through the LLDPE geomembrane using POLLUTE and the P_g values calculated from Eqs. (R2) and (R3) overpredicts the experimental observations. PFOA modelling using the P_g = 2.0 × 10^{-12} m^2/s, calculated from Eq. R(2), predicted that the PFOA source and receptor concentrations would reach equilibrium at approximately 150 days (Fig. 6). Similarly using P_g = 5.5 × 10^{-12} m^2/s from Eq. (2) for PFOS would predict that concentrations would reach equilibrium at approximately 60 days. However, in reality there was no measurable change in the source concentration of either PFOA or PFOS and barely detectable concentrations in the receptor after 483 days and hence the predicted values form R2 are not correct. At the other extreme, Eq. (R3) gives P_g = 6.5 × 10^{-106} m^2/s (PFOA) and P_g = 9.4 × 10^{-170} m^2/s (PFOS). These P_g values are more than 90 orders of magnitude lower than those calculated using Eq. (R2). POLLUTE modelling of the experiments using P_g = 6.5 × 10^{-106} m^2/s ($P_g = D_g$, S_{gf} = 1) for PFOA (c_o = 19.8 mg/L) and P_g = 9.4 × 10 $^{-170}$ m^2/s ($P_g = D_g$, S_{gf} = 1) for PFOS (c_o = 22.7 mg/L), predicts receptor concentrations of < 10^{-48} mg/L for both contaminants at 1500 days. Since PFOA and PFOS have been detected in the receptors before and at 483 days, these values cannot be even close.

Eq. (R4), gave D_g = 1.4 × 10^{-16} m^2/s (PFOA) and D_g = 7.4 × 10^{-16} m^2/s (PFOS) based on the compounds' log K_{ow}. These values are the closest to the best estimates deduced from the experiments compared to the P_g and S_{gf} values calculated using Eqs. (R1), (R2), and (R3). POLLUTE modelling of the experiment using D_g = 1.4 × 10^{-16} m^2/s (PFOA; $P_g = D_g$, S_{gf} = 1), Fig. 6, and D_g = 7.4 × 10^{-16} m^2/s (PFOS; $P_g = D_g$, S_{gf} = 1) predicted receptor concentrations of 87 µg/L (PFOA) and 138 µg/L (PFOS) at 483 days, compared to the analyzed concentrations of 0.3 µg/L (PFOA) and 0.5 µg/L (PFOS). Thus, the parameters estimated with this approach are quite conservative and over predict the observed receptor concentrations by more than two orders of magnitude at 483 days. A value of S_{gf} = 1 was used when modelling using the D_g calculated from Eq. (R4) because the S_{gf} predicted by Eq. (R1) was too high to be applicable.

The modelling of the experiments using the current best estimates of P_{gPFOA} = 3.1 × 10^{-17} m^2/s and P_{gPFOS} = 1.6 × 10^{-16} m^2/s predicted receptor concentrations of the 0.1 mm LLDPE at 23 °C, at 1500 days, will be 8.0 µg/L for PFOA (c_o = 19.8 mg/L; c/c_o = 4 × 10^{-4}) (Fig. 6) and 57.6 µg/L (PFOS c_o = 22.7 mg/L; c/c_o = 2.5 × 10^{-3}). Predicted receptor values using (R2), (R3), and (R4) for PFOA and PFOS at 483 days are given in Supplementary Material Table S3 for 0.1 mm LLDPE.

The authors hypothesize that the low permeation of PFOA and PFOS is related to the molecular weight, acidic nature, and surfactant properties of the contaminants. The molecular weights of the contaminants are 414.07 g/mol (PFOA) and 500.13 g/mol (PFOS), which are greater than the molecular weights of BTEX (78.11–106.16 g/mol), PCBs (291.98 g/mol), BPA (228.29 g/mol), and phenol (94.11 g/mol) and comparable to PBDE (564.7 g/mol). The estimated P_g of PBDE is 7.2 × 10^{-9} m^2/s, however it is difficult to directly compare the diffusion behaviour of PFOA and PFOS to PBDE as the extremely high partitioning coefficient controls the P_g. PFOA and PFOS are considered very strong acids, and the compounds have estimated pK_a values of −0.2 (PFOA) and −3.3 (PFOS)

Table 3
Comparison PFOA and PFOS best estimate D_g, S_{gf}, and P_g values LLDPE to values calculated using relationships presented by Sangam and Rowe (2001).

	PFOA	PFOS
D_g (This study)	<2.5 × 10^{-17} m^2/s	<4 × 10^{-17} m^2/s
S_{gf} (This study)	0.9–1.4	2.8–5.3
P_g (This study)	<3.1 × 10^{-17} m^2/s	<1.6 × 10^{-16} m^2/s
[R1] $\log S_{gf} = -1.1523 + 1.2355(\log K_{ow})$	S_{gf} = 61,000	S_{gf} = 25,000
[R2] $\log P_g = -13.4476 + 2.2437(\log K_{ow}) - 0.3910(\log K_{ow})^2$	P_g = 2.0 × 10^{-12} m^2/s	P_g = 5.5 × 10^{-12} m^2/s
[R3] $\log P_g = -25.6933 + 0.2633 M_W - 1.0995 \times 10^{-3}(M_W)^2$	P_g = 6.6 × 10^{-106} m^2/s	P_g = 9.4 × 10^{-170} m^2/s
[R4] $\log D_g = -12.3624 + 0.9205 \log K_{ow} - 0.3424(\log K_{ow})^2$	D_g = 1.4 × 10^{-16} m^2/s	D_g = 7.4 × 10^{-16} m^2/s

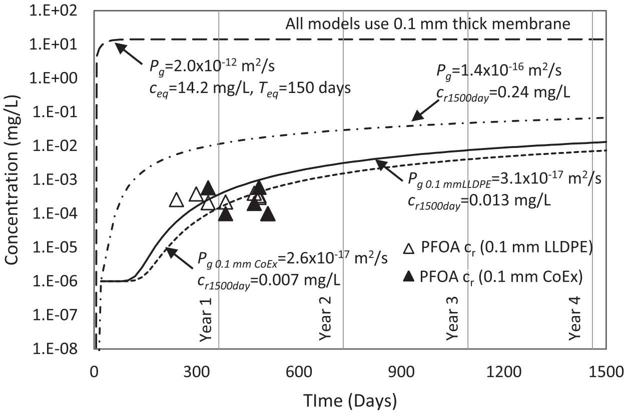

Fig. 6. Experimental PFOA concentrations for 0.1 mm LLDPE and 0.1 mm CoEx, and predicted PFOA receptor concentrations for D_g = 2.5 × 10^{-17} m^2/s S_{gf} = 1.4 P_g = 3.1 × 10^{-17} m^2/s (0.1 mm LLDPE), D_g = P_g = 2.6 × 10^{-17} m^2/s S_{gf} = 1 (0.1 mm CoEx), P_g = D_g = 2.0 × 10^{-12} m^2/s [Eq. (R2)], and P_g = D_g = 1.4 × 10^{-16} m^2/s [Eq. (R4)]. Predicted receptor concentration for P_g = 6.6 × 10^{-106} m^2/s (Eq. (R3)] at 1500 days is < 1 × 10^{-48} mg/L and is not shown.

(Deng et al., 2012). The aqueous source pH (c_o ~ 20 mg/L) ranged from 3.83 to 4.05, as measured using a pH probe, and the PFOA and PFOS are likely to be in a dissociated form in these tests and in the environment, as reported pH values in landfill leachate range from 5.9 to 8.5 in municipal solid waste (Bonaparte et al., 2002; Rowe et al., 2004). Limited partitioning of PFOA and PFOS due to their acidic nature is consistent with experiments using acetic acid with polypropylene and polyethylene membranes, where negligible sorption of the acetic acid to the geomembranes was observed (Aminabhavi and Naik, 1998). The surfactant properties of these contaminants result in hydrophilic and lipophilic characteristics; the hydrophilic nature of these contaminants could be a possible explanation for the low partitioning of the contaminants from an aqueous solution into the geomembrane.

As discussed, the LLDPE (and likely HDPE) and CoEx geomembranes are both extremely effective diffusive barriers to PFOA and PFOS. However, landfill leachates contain a variety of hydrocarbons, such as BTEX, in addition to PFAS, and polyethylene has lower diffusive resistance to BTEX than geomembranes coextruded with EVOH that have a P_g orders of magnitude lower than for LLDPE (DiBattista and Rowe, 2020; Eun et al., 2017; Jones and Rowe, 2016; McWatters and Rowe, 2010, 2018; Rowe et al., 2004). In addition to low permeation of PFOA and PFOS, membranes coextruded with EVOH have the benefit of additional superior diffusive resistance to other contaminants, like BTEX, found in landfill leachates.

6. Conclusions

Diffusion and partitioning of PFOA and PFOS with respect to LLDPE and LLDPE coextruded with EVOH was investigated for concentrations above and below 0.001 CMC at 23 °C, 35 °C, and 50 °C using diffusion testing and sorption vial testing (LLDPE only). The following conclusions were developed; these conclusions are preliminary as only very low concentrations and no consistent trend were detected throughout the 509 day monitoring period. For the materials and conditions tested, these preliminary conclusions are:

1. Testing demonstrated very limited diffusion through both the coextruded geomembranes with an EVOH core and the LLDPE geomembranes. While both types of membranes exhibit low diffusivity of PFOA and PFOS, the coextruded geomembranes with an EVOH core (CoEx) performed better in all test where a direct comparison could be made while, the literature also shows that the coextruded geomembranes with an EVOH core has the added benefit of being a superior barrier to organic contaminants (e.g., BTEX) present in landfill leachate.
2. It is unlikely that hemi-micelle and micelle formation, if present, affected the diffusion properties of the membranes, as similar behaviour was observed in experiments with c_o > 20-mg/L and c_o = 1.1 mg/L.
3. Results from the sorption test vials indicated limited partitioning of contaminants to LLDPE, and S_{gf} values of 0.9–1.4 (PFOA) and 2.8–5.3 (PFOS) were calculated from these tests. Diffusion experiments did not exhibit detectable decreases in source concentration, confirming that minimal partitioning of the contaminants to the polyethylene is occurring and consistent with theoretical predictions based on the best estimate diffusion and permeation parameters.
4. At the last sampling event before writing this paper, receptor contaminant concentrations were 0.3 μg/L (PFOA) and 0.5 μg/L (PFOS) for the 23 °C 0.1 mm LLDPE (483 days) and below detection for PFOA and 3.7 μg/L for PFOS for the 0.1 mm CoEx (at 509 days). This resulted in best estimates of P_g of ≤3.1 × 10^{-17} m^2/s (PFOA) and ≤1.6 × 10^{-16} m^2/s (PFOS) for LLDPE and P_g values of ≤ 2.6 × 10^{-17} m^2/s (PFOA) and ≤5.5 × 10^{-17} m^2/s (PFOS) for the 0.1 mm CoEx. These values have been deduced using the data available, and it is likely that they will be further refined with time. Permeation coefficient, P_g values deduced for the 0.75 mm LLDPE at various temperatures ranged from ≤6.8 × 10^{-16} m^2/s (PFOS, 0.75 mm CoEx at 23 °C) to ≤5.2 × 10^{-15} m^2/s (PFOS, 0.75 mm LLDPE at 50 °C).
5. When compared to existing diffusion and partitioning coefficient estimates of BTEX, PBDE, BPA, and PCBs, the diffusion of PFOA and PFOS is most comparable to BPA, where limited partitioning and diffusion through the membranes was observed during the monitoring. Relationships to predict D_g, S_{gf}, and P_g, as proposed by Sangam and Rowe (2001) do not adequately capture the behaviour of PFOA and PFOS. It is likely that the high molecular weights and surfactant nature of these molecules result in extremely low P_g values for LLDPE.

For landfills containing PFOA and PFOS as well as volatile organic contaminants (e.g., BTEX, TCE, PCE etc.) that could impact groundwater by diffusion through an unsaturated zone between a single GMB/GCL composite liner and an aquifer, an overarching conclusion is that by the use of a co-extruded 1.5 mm GMB with an EVOH core (as has been used to contain hydrocarbon contaminated soil in Antarctica; McWatters et al., 2016) deserves more consideration than it has been given in the past.

These conclusions are specific to diffusive contaminant transport only and are based on the data available. These conclusions do not account for other factors that may affect contaminant transport through geomembranes (e.g., holes in the geomembrane, aging, etc.)

This study did not consider the depletion of antioxidants from, or the effect of the PFAS on, the service-life of the either the LLDPE or coextruded geomembranes. Aging studies of HDPE using leachate constituents found that the presence of surfactants in the leachate resulted in reductions of standard and high pressure oxidative inductive times as the geomembrane aged (Abdelaal et al., 2014). If the surfactant properties of PFOA and PFOS result in similar antioxidant depletion, an additional benefit of geomembranes with coextruded EVOH cores could be protection of the receptor facing polyethylene from antioxidant depletion. This is a hypothesis that requires additional experimentation and study to confirm.

Declaration of Competing Interest

The authors declare that they have no known competing financial interests or personal relationships that could have appeared to influence the work reported in this paper.

Acknowledgements

This study is was financially supported by Kuraray America Inc., who also provided materials for testing, and the authors are grateful for their support. Additionally, the authors would like to thank Dr. A. Rutter and the Analytical Services Unit at Queen's University, for their support and use of laboratory facilities.

Data availability statement

The data used during the study is available from the first author upon request, and models used in analysis is commercially available from GAEA Technologies Ltd.

Appendix A. Supplementary material

Supplementary data to this article can be found online at https://doi.org/10.1016/j.wasman.2020.07.036.

References

3M Company, 1999a. The Science of Organic Fluorochemistry.

3M Company, 1999b. Fluorochemical Use, Distribution and Release Overview.

3M Company, 2000. Phase-out Plan for POSF-Based Products. St. Paul, MN.

Abdelaal, F.B., Rowe, R.K., Islam, M.Z., 2014. Effect of leachate composition on the long-term performance of a HDPE geomembrane. Geotext. Geomembr. 42 (4), 348–362.

Aminabhavi, T.M., Naik, H.G., 1998. Chemical compatibility testing of geomembranes – sorption/desorption, diffusion, permeation and swelling phenomena. Geotext. Geomembr. 16 (6), 333–354.

Arp, H.P.H., Niederer, C., Goss, K.-U., 2006. Predicting the partitioning behavior of various highly fluorinated compounds. Environ. Sci. Technol. 40 (23), 7298–7304.

August, H., Tatzky, R., 1984. Permeabilities of commercially available polymeric liners for hazardous landfill leachate organic constituents. In: International Conference on Geomembranes, pp. 163–168.

Barone, F.S., Rowe, R.K., Quigley, R.M., 1990. Laboratory determination of chloride diffusion coefficient in an intact shale. Can. Geotech. J. 27 (2), 177–184.

Barone, F.S., Rowe, R.K., Quigley, R.M., 1992a. Estimation of chloride diffusion coefficient and tortuosity factor for mudstone. J. Geotech. Eng. 118 (7), 1031–1045.

Barone, F.S., Rowe, R.K., Quigley, R.M., 1992b. A laboratory estimation of diffusion and adsorption coefficients for several volatile organics in a natural clayey soil. J. Contam. Hydrol. 10 (3), 225–250.

Benskin, J.P., Li, B., Ikonomou, M.G., Grace, J.R., Li, L.Y., 2012. Per-and polyfluoroalkyl substances in landfill leachate: patterns, time trends, and sources. Environ. Sci. Technol. 46, 11532–11540.

Bonaparte, R., Daniel, D., Koerner, R.M., 2002. Assessment and recommendations for improving the performance of waste containment systems.

Buck, R.C., Franklin, J., Berger, U., Conder, J.M., Cousins, I.T., Voogt, P. De, Jensen, A.A., Kannan, K., Mabury, S.A., van Leeuwen, S.P.J., 2011. Perfluoroalkyl and polyfluoroalkyl substances in the environment: Terminology, classification, and origins. Integr. Environ. Assess. Manage. 7 (4), 513–541.

Busch, J., Ahrens, L., Sturm, R., Ebinghaus, R., 2010. Polyfluoroalkyl compounds in landfill leachates. Environ. Pollut. 158, 1467–1471.

Crank, J., 1979. The Mathematics of Diffusion. Oxford University Press.

Deng, S., Zhang, Q., Nie, Y., Wei, H., Wang, B., Huang, J., Yu, G., Xing, B., 2012. Sorption mechanisms of perfluorinated compounds on carbon nanotubes. Environ. Pollut. 168, 138–144.

Di Battista, V., Rowe, R.K., 2020. Contaminant diffusion through a novel coextruded vapour barrier. J. Geotech. Geoenviron. Eng. (in press)

Eggen, T., Moeder, M., Arukwe, A., 2010. Municipal landfill leachates: A significant source for new and emerging pollutants. Sci. Total Environ. 408, 5147–5157.

Eun, J., Tinjum, J.M., Benson, C.H., Edil, T.B., 2017. Comparison of volatile organic compound transport in composite liners with HDPE and ethylene-vinyl alcohol co-extruded geomembranes. J. Geotech. Geoenviron. Eng. 143 (6), 1–11.

Fuertes, I., Gómez-Lavín, S., Elizalde, M.P., Urtiaga, A., 2017. Perfluorinated alkyl substances (PFASs) in northern Spain municipal solid waste landfill leachates. Chemosphere 168, 399–407.

Gallen, C., Drage, D., Eaglesham, G., Grant, S., Bowman, M., Mueller, J.F., 2017. Australia-wide assessment of perfluoroalkyl substances (PFASs) in landfill leachates. J. Hazard. Mater. 331, 132–141.

Government of Canada, 2012. Proposed Risk Managment Approach for Perfluorooctanoic Acid (PFOA), its Salts, and its Precursors and Long-Chain (C9-C20) Perfluorocarboxylic Acids (PFCAs), their Salts, and their Precursors.

Hale, S.E., Arp, H.P.H., Slinde, G.A., Wade, E.J., Bjørseth, K., Breedveld, G.D., Straith, B. F., Moe, K.G., Jartun, M., Høisæter, Å., 2017. Sorbent amendment as a remediation strategy to reduce PFAS mobility and leaching in a contaminated sandy soil from a Norwegian firefighting training facility. Chemosphere 171, 9–18.

Health Canada, 2018a. Guidelines for Canadian Drinking Water Quality: Guideline Technical Document — Perfluorooctane Sulfonate (PFOS). Ottawa, Ontario.

Health Canada, 2018b. Guidelines for Canadian Drinking Water Quality Guideline Technical Document Perfluorooctanoic Acid (PFOA). Ottawa, ON.

Islam, M.Z., Rowe, R.K., 2009. Permeation of BTEX through unaged and aged HDPE geomembranes. J. Geotech. Geoenviron. Eng., 1130–1140

Johnson, R.L., Anschutz, A.J., Smolen, J.M., Simcik, M.F., Penn, R.L., 2007. The adsorption of perfluorooctane sulfonate onto sand, clay, and iron oxide surfaces. J. Chem. Eng. Data 52 (4), 1165–1170.

Jones, D., 2016. Containment of Organic Contaminants using Geosynthetics. Queen's University.

Jones, D.D., Rowe, R.K., 2016. BTEX migration through various geomembranes and vapor barriers. J. Geotech. Geoenviron. Eng. 142 (10), 1–12.

Lagaron, J.M., Powell, A.K., Bonner, G., 2001. Permeation of water, methanol, fuel and alcohol-containing fuels in high-barrier ethylene-vinyl alcohol copolymer. Polym. Test. 20, 569–577.

Lake, C.B., Rowe, R.K., 2004. Volatile organic compound diffusion and sorption coefficients for a needle-punched GCL. Geosynth. Int. 11 (4), 257–272.

Martin, J.W., Asher, B.J., Beesoon, S., Benskin, J.P., Ross, M.S., 2010. PFOS or PreFOS? Are perfluorooctane sulfonate precursors (PreFOS) important determinants of human and environmental perfluorooctane sulfonate (PFOS) exposure? J. Environ. Monit.

McWatters, R.S., 2010. Diffusive Transport of Volatile Organic Compounds through Geomembranes. Queen's University.

McWatters, R.S., Rowe, R.K., 2009. Transport of volatile organic compounds through PVC and LLDPE geomembranes from both aqueous and vapour phases. Geosynth. Int. 16 (6), 468–481.

McWatters, R.S., Rowe, R.K., 2010. Diffusive transport of VOCs through LLDPE and two coextruded geomembranes. J. Geotech. Geoenviron. Eng. 136 (September), 1167–1177.

McWatters, R.S., Rowe, R.K., 2014. Permeation of volatile organic compounds through EVOH thin film membranes and coextruded LLDPE/EVOH/LLDPE geomembranes. J. Geotech. Geoenviron. Eng., 1–14

McWatters, R.S., Rowe, R.K., 2018. Barrier permeation properties of EVOH thin-film membranes under aqueous and non-aqueous conditions. Geotext. Geomembr. 46 (4), 529–541.

McWatters, R.S., Rowe, R.K., Wilkins, D., Spedding, T., Hince, G., Richardson, J., Snape, I., 2019. Modelling of vapour intrusion into a building impacted by a fuel spill in Antarctica. J. Environ. Manage. 231, 467–482.

McWatters, R.S., Rowe, R.K., Wilkins, D., Spedding, T., Jones, D., Wise, L., Mets, J., Terry, D., Hince, G., Gates, W.P., Di Battista, V., Shoaib, M., Bouazza, A., Snape, I., 2016. Geosynthetics in Antarctica: Performance of a composite barrier system to contain hydrocarbon-contaminated soil after three years in the field. Geotext. Geomembr. 44 (2016), 673–685.

Milley, S.A., Koch, I., Fortin, P., Archer, J., Reynolds, D., Weber, K.P., 2018. Estimating the number of airports potentially contaminated with perfluoroalkyl and polyfluoroalkyl substances from aqueous film forming foam: A Canadian example. J. Environ. Manage. 222, 122–131.

Montgomery, J.H., Welkom, L.M., 1989. Groundwater Chemicals Desk Reference. Lewis Publishers Inc., Chelsea, MI.

National Institute of Health Sciences, 2020. Pefluoroalkyl and Polyfluoroalkyl Substances (PFAS). https://www.niehs.nih.gov/health/topics/agents/pfc/index.cfm (Mar. 24, 2020).

Park, J.K., Hoopes, J.A., Sakti, J.P., 1995. Effectiveness of Geomembranes as Barriers for Organic Compounds. Industrial Fabrics Association International, St. Paul, MN (United States).

Park, J.K., Nibras, M., 1993. Mass flux of organic chemicals through polyethylene geomembranes. Water Environ. Res. 65 (3), 227–237.

Rayne, S., Forest, K., 2009. A comparative assessment of octanol-water partitioning and distribution constant estimation methods for perfluoroalkyl carboxylates and sulfonates. Nature Precedings. Springer Science and Business Media LLC.

Rowe, R.K., 1998. Geosynthetics and the minimization of contaminant migration through barrier systems beneath solid waste. In: Sixth International Conference on Geosynthetics, Atlanta, GA, 76.

Rowe, R.K., 2015. Reflections on the evolution of geoenvironmental engineering. Environ. Geotech. 2 (2), 65–67.

Rowe, R.K., Badv, K., 1996. Advective-diffusive contaminant migration in unsaturated sand and gravel. J. Geotech. Eng. 122 (12), 965–975.

Rowe, R.K., Booker, J.R., 1985. Two-dimensional pollutant migration in soils of finite depth. Can. Geotech. J. 22 (4), 429–436.

Rowe, R.K., Booker, J.R., 2004. POLLUTE vol 7–1D Pollutant Migration through a Non-homogenous Soil. GAEA Environmental Engineering Ltd..

Rowe, R.K., Booker, J.R., Fraser, J., 1997. POLLUTE v. 6.3: 1D pollutant migration through a non-homogeneous soil. Distributed by GAEA Environmental Ltd. Whitby, Ontario.

Rowe, R.K., Caers, C.J., Barone, F., 1988. Laboratory determination of diffusion and distribution coefficients of contaminants using undisturbed clayey soil. Can. Geotech. J. 25 (1), 108–118.

Rowe, R.K., Jones, D.D., Rutter, A., 2016a. Polychlorinated biphenyl diffusion through HDPE geomembrane. Geosynth. Int. 23 (6), 408–421.

Rowe, R.K., Mukunoki, T., Bathurst, R.J., Rimal, S., Hurst, P., Hansen, S., 2005. The performance of a composite liner for retaining hydrocarbons under extreme environmental conditions. In: Slopes and Retaining Structures Under Seismic and Static Conditions, American Society of Civil Engineers, Reston, VA, 1–17.

Rowe, R.K., Quigley, R.M., Brachman, R.W.I., Booker, J.R., 2004. Barrier Systems for Waste Disposal Facilities. E & FN Spon, New York, NY.

Rowe, R.K., Saheli, P.T., Rutter, A., 2016b. Partitioning and diffusion of PBDEs through an HDPE geomembrane. Waste Manage. 55, 191–203.

Saheli, P.T., Rowe, R.K., Rutter, A., 2016. Diffusion of bisphenol-A (BPA) through an HDPE geomembrane. Geosynth. Int. 23 (6), 452–462.

Sangam, H.P., Rowe, R.K., 2001. Migration of dilute aqueous organic pollutants through HDPE geomembranes. Geotext. Geomembr. 19 (6), 329–357.

Sangam, H.P., Rowe, R.K., 2005. Effect of surface fluorination on diffusion through an HDPE geomembrane. ASCE Journal of Geotechnical and Geoenvironmental Engineering, 131 (6), 694–704.

US EPA, 2012. Estimation Programs Interface Suite(TM) for Microsoft Windows, v4.11. United States Environmental Protection Agency, Washington, DC.

Yan, H., Cousins, I.T., Zhang, C., Zhou, Q., 2015. Perfluoroalkyl acids in municipal landfill leachates from China: Occurrence, fate during leachate treatment and potential impact on groundwater. Sci. Total Environ. 524–525, 23–31.

Yu, Q., Zhang, R., Deng, S., Huang, J., Yu, G., 2008. Sorption of perfluorooctane sulfonate and perfluorooctanoate on activated carbons and resin: Kinetic and isotherm study. Water Res. 43, 1150–1158.